A Simple Field-Theoretic Simulation Method for Compressible Block Copolymer Systems

Junhan Cho* and Zhen-Gang Wang

Department of Polymer Science and Engineering, and Hyperstructured Organic Materials Research Center, Dankook University, San-8, Hannam-dong, Yongsan-gu, Seoul, 140-714, Korea, and Department of Chemical Engineering, California Institute of Technology, Pasadena, California 91125

Received December 1, 2005; Revised Manuscript Received April 20, 2006

ABSTRACT: A simple field-theoretic simulation method based on a compressible random-phase approximation (RPA) theory has been suggested to understand the self-assembly behavior and its pressure responses of compressible block copolymer systems. Finite compressibility is incorporated in the free energy functional for the dissipative dynamics through effective RPA interactions that account for the excluded volume and the attractive nonbonded interactions. It was shown that basic equation-of-state parameters completely characterizing given block components readily yield stable and metastable morphologies without any presumed symmetry over a wide range of temperature−pressure−composition space for copolymer melts in unconfined or confined geometry. It was demonstrated that the simulation tool is capable of predicting in a unified way block copolymer phase behavior, not only exhibiting nanoscale ordering either upon cooling or reversely upon heating, but also revealing barotropicity and baroplasticity.

Introduction

Phase-segregating block copolymers from two or more homopolymers have been known to exhibit nanoscale self-assembly behavior to form microscopically ordered structures. A number of such ordered structures have been identified up to now. There are classical morphologies such as body-centered cubic spheres (bcc), hexagonally packed cylinders (hex), and lamellar (lam) structures. Recently found morphologies such as bicontinuous gyroid, hexagonally perforated lamellae, and the latest orthorhombic 3-fold structures are categorized as complex morphologies. [1−5] A transition from a disordered state to an ordered state is induced either upon cooling or upon heating, where the former is called the upper order−disorder transition (UODT) and the latter the lower disorder−order transition (LDOT). The UODT behavior, which is analogous to upper critical solution temperature (UCST) behavior in polymer blends, is driven by the unfavorable energetics between dissimilar monomers comprising a given block copolymer.[1−4] As an analogue to lower critical solution temperature (LCST) behavior in the blends, the LDOT behavior is, on the contrary, of entropic origin. The difference in volume fluctuations or the entropic penalty in forming specific interactions is considered to be the source of the LDOT.[6,7] Studies on the phase behavior of block copolymers have drawn much interest theoretically and experimentally because of their usage in a variety of applications such as elastomers, compatibilizers, surface modifiers, and in lithography, patterning, displays, etc.[4,8]

There have been in recent decades extensive theoretical developments to analyze the microphase separation behavior and transitions between equilibrium microstructures for molten block copolymers or systems containing block copolymers in a weak-to-strong segregation regime.[4] The most influential among them are Leibler's Landau approach[9] and its fluctuation corrections[10−12] in a weak segregation regime, Helfand's self-consistent field theory (SCFT) in a strong segregation regime,[13] and the subsequent improvements on the SCFT in all segregation levels.[14−16] However, almost all of the theories for block copolymers presume the symmetry of ordered patterns and compare the calculated free energies to determine equilibrium structures and transition conditions. There have been efforts through field-theoretic simulation approaches to predict a priori morphology to which a phase segregating block copolymer evolves.[17] Phenomenological cell dynamics simulations by Oono and co-workers have been widely used to describe phase separation kinetics in various mixtures, including block copolymers with a free energy expansion suitable for a given mixture system.[18−22] However, this method possesses such a definite drawback that there is no systematic way to adjust phenomenological parameters necessary for the simulation runs. Fraaije then developed a dynamic density functional theory (DDFT) from the generalized time-dependent Ginzburg−Landau theory to simulate short copolymer systems that are connected to real systems.[23−26] Fredrickson and co-workers introduced the computational screening method, using the SCFT equations to assign stable and metastable morphologies at given thermodynamic variables in the mean-field level.[17,27,28] Later, Bohbot-Raviv and Wang introduced a simple Landau-type free energy functional with a local ideal Flory−Huggins free energy as a reference and its truncated expansion compensating for the adopted reference free energy.[29] The latter three methods were able to demonstrate a priori estimation of stationary morphologies for molten multiblock or star copolymers with a large parameter space of interaction pairs and compositions and also for block copolymers in confined geometry.[17,27,29−36] Recently, Uneyama and Doi presented a simulation method based on a density functional theory, which is similar to Bohbot-Raviv and Wang's approach, but suggests improvement in a better description of mixture phase behavior in the strong segregation regime.[37,38]

Most of the block copolymer theories developed so far are based on the common assumption of system incompressibility. Pressure, though it is an equally important thermodynamic variable as temperature, has been disregarded in those field theories. However, there have been numerous findings that strongly address a clear need for finite compressibility to interpret the compressible nature and the pressure effects of

* Corresponding author. E-mail: jhcho@dku.edu.

10.1021/ma052565r CCC: $33.50
Published on Web 05/27/2006

block copolymers. A decade ago, Russell and co-workers discovered LDOT phenomena in styrenic block copolymer melts and films.[6,39,40] Later, they reported large increases in order−disorder transition temperatures upon pressurization in those LDOT systems.[41,42] Schwahn and co-workers reported anomalous responses of some UODT block copolymers to pressure.[43−45] It was observed by them that pressure suppresses order−disorder transitions or even yields the nonmonotonic responses of transitions in some cases. Mayes and co-workers then brought a concept of baroplasticity to the block copolymer society to utilize the pressure-induced suppression of ordering in material fabrication.[46] These phenomena culminated in the discovery of highly pressure-sensitive loop-forming diblock copolymers with both LDOT and UODT by Ryu, Kim, and Russell.[47,48] The LDOT and the pressure effects, including baroplasticity, have been successfully interpreted in a recent series of works by the one of the present authors on the analytical Landau analysis and its fluctuation corrections for compressible block copolymers, which are based on a compressible random-phase approximation (RPA) theory.[49−56] Finite compressibility was incorporated into the theory through effective RPA interactions, which is obtained from an off-lattice equation-of-state model by Cho and Sanchez (CS).[49,57] Both the excluded volume interactions and nonbonded attractive interactions are included in the RPA interactions. Equilibrium microphase morphologies and transition conditions were determined in a more general temperature−pressure−composition space. However, this analytical theory also possesses the restriction to require the predetermined symmetry as other theories do.

It is our objective here to overcome such a limitation of the analytical theory, at least in the mean-field level, by introducing a simple field-theoretic simulation technique for the compressible copolymer systems. The simulation method for incompressible systems devised by Bohbot-Raviv and Wang[29] is generalized to be combined with the compressible RPA. Helfand included in his original SCFT a primitive contribution from finite compressibility with the harmonic density fluctuations term.[13] Fraaije and co-workers modified their DDFT to simulate compressible block copolymers by adding a correction factor from the athermal chain connectivity as the excluded volume contributions to the free energy functional.[24] Helfand's harmonic penalty term was also tested in the modification of DDFT. [24,26] Our theory, which is based on the compressible RPA, directly inputs the effective interaction fields with the excluded volume and the attractive nonbonded interactions into the correlation functions and the free energy functional.[58] Therefore, basic equation-of-state parameters completely characterizing given block components, such as monomer sizes, chain sizes, and self- and cross-contact interactions, readily lead to stable or metastable morphologies without any presumed symmetry once a thermodynamic condition is set. We thus consider that the compressible character of block copolymers can be more elaborately described in the present theory than other approaches.

Theory

In this section, we will present an approximate free energy functional for a simple field-theoretic simulation method that is suitable for compressible block copolymer systems. Consider a system of ABC... multiblock copolymers with N_i monomers of the ith component, where $i = 1, 2, 3, ...$, correspond to A, B, C, ..., respectively, to have the overall size N ($= \sum_i N_i$). All the monomers are assumed to have the identical diameter σ. The close-packed volume fraction ϕ_i of the ith component is then defined as $\phi_i \equiv N_i/N$. The system is allowed to be compressible: there is free volume in the system. We denote as η_i the global packing density of i monomers that implies the fraction of system volume occupied by all the monomers of the ith component. The $\eta_i(\vec{r})$ represents the local packing density of such monomers at a position $\vec{r}$. Phase segregation in the system can be probed by considering the average packing density fluctuations, or the order parameter ψ_i, for the i monomers. The order parameter ψ_i is defined as $\psi_i(\vec{r}) \equiv \langle \delta\eta_i(\vec{r})\rangle = \langle \eta_i(\vec{r}) - \eta_i\rangle$, where the brackets imply the thermal average. In a Landau mean-field approach, the free energy F for the system can be expanded as a series in the order parameter ψ_i as[50,51,53]

$$\beta(F - F_0) = \sum_{m=2}^{\infty} \frac{1}{m!} \int \mathrm{d}\vec{q}_1 \cdots \mathrm{d}\vec{q}_m \Gamma^{(m)}_{i_1 \cdots i_m}(\vec{q}_1, \cdots, \vec{q}_m)\psi_{i_1}(\vec{q}_1) \cdots \psi_{i_m}(\vec{q}_m) \tag{1}$$

where the F_0 implies the free energy in a disordered state and $\beta = 1/kT$ has its usual meaning. In the above equation, $\psi_i(\vec{q})$ is the Fourier transform of $\psi_i(\vec{r})$ as $\psi_i(\vec{q}) = \int \mathrm{d}\vec{r}\psi_i(\vec{r})e^{i\vec{r}\cdot\vec{q}}$, with $\vec{q}$ denoting physically the scattering vector. The coefficient $\Gamma^{(m)}_{i_1 \cdots i_m}$ is commonly known as the mth-order vertex function. It is well-known that $\Gamma^{(2)}_{ij}(\vec{q}_1, \vec{q}_2) = S_{ij}^{-1}(\vec{q}_1, \vec{q}_2)\,\delta(\vec{q}_1 + \vec{q}_2)$, where S_{ij} is the second-order monomer−monomer correlation function and $\delta(\vec{q}_1 + \vec{q}_2)$ is the Dirac delta function. The free energy in eq 1 can be approximately written by using the local ideal free energy functional F_{id} and its mth order expansion $F^{(m)}_{\mathrm{id}}$ as[29]

$$\beta(F - F_0) \cong \beta[F_{\mathrm{id}} - F^{(m)}_{\mathrm{id}}] + \frac{1}{2}\int \mathrm{d}\vec{q}[S_{ij}^{-1}(\vec{q})]\psi_i(\vec{q}) \times \psi_j(-\vec{q}) + \sum_{k=3}^{m} \frac{1}{k!} \int \Gamma^{(k)}_{i_1 \cdots i_k} \prod_{l=1}^{k} \psi_{i_l}(\vec{q}_l)\,\mathrm{d}\vec{q}_l \tag{2}$$

where the suitable functional form of F_{id} for compressible block copolymers can be given as

$$\beta F_{\mathrm{id}} = \frac{R_g^{\,3}}{v^*} \int \frac{\mathrm{d}\vec{r}}{R_g^{\,3}} \sum \frac{\langle \eta_i(\vec{r})\rangle}{N_i} \ln\langle \eta_i(\vec{r})\rangle \tag{3}$$

In eq 3, v^* ($= \pi\sigma^3/6$) is the volume of one monomer, and R_g is the unperturbed gyration radius of the copolymer. The F_{id} is expanded as

$$\beta F_{\mathrm{id}} = \frac{R_g^{\,3}}{v^*} \int \frac{\mathrm{d}\vec{r}}{R_g^{\,3}} \sum \left\{ \frac{\eta_i}{N_i} \ln \eta_i + \frac{1 + \ln \eta_i}{N_i} \cdot \psi_i(\vec{r}) + \frac{1}{2}\frac{\psi_i(\vec{r})^2}{N_i \eta_i} + \cdots \right\} \tag{4}$$

The simplest free energy functional can then be given as

$$\beta(F - F_0) \cong \beta[F_{\mathrm{id}} - F^{(2)}_{\mathrm{id}}] + \frac{1}{2}\int \mathrm{d}\vec{q}[S_{ij}^{-1}(\vec{q})]\psi_i(\vec{q})\psi_j(-\vec{q}) \tag{5}$$

Equation 5 is particularly useful for block copolymer systems with three or more components because the higher-order vertex functions than $\Gamma^{(2)}_{ij}$ is generally not known in such cases. The present work will only employ the simplest eq 5 for simulations.

According to the compressible RPA by Cho,[49−55] the inverse correlation functions for compressible systems can be ap-

proximated as

$$S_{ij}^{-1} = S_{ij}^{0-1} + \frac{1}{v^*}\beta W_{ij} \tag{6}$$

where S_{ij}^0's are the Gaussian correlation functions for given copolymers. The conventional Gaussian functions for the corresponding incompressible copolymers are equated here to $v^*S_{ij}^0/\eta$, where η corrects the diluted contact probabilities by the presence of free volume. In eq 6, the effective interaction field W_{ij} is obtained from the free energy F_0 of the CS equation-of-state model. The CS free energy is given as $F_0 = F_0^{id} + F_0^{EV} + U^{nb}$. The F_0^{id} represents the ideal free energy of the noninteracting Gaussian chain system. The F_0^{EV} and U^{nb} stand for the contribution to the free energy from the excluded volume effects and the attractive interactions between nonbonded monomers, respectively. The W_{ij} is formulated as the second-order derivative of the nonideal part of the CS free energy per system volume V with respect to η's as

$$\beta W_{ij}/v^* = \partial^2[(\beta F_0^{EV} + \beta U^{nb})/V]/\partial\eta_i\partial\eta_j \tag{7}$$

The contributions from F_0^{EV} and U^{nb} in eq 7 are respectively denoted as L_{ij}/v^* and $[-\beta\epsilon_{ij}^{app}]/v^*$, where these two are properly written as follows:

$$L_{ij}(\eta) = \frac{3}{2}\left[\frac{4}{(1-\eta)^3} + \frac{6\eta}{(1-\eta)^4} - \left(2 - \frac{1}{N_i} - \frac{1}{N_j}\right)\frac{1}{(1-\eta)^2} - \left(1 - \sum\frac{\phi_i}{N_i}\right)\frac{2\eta}{(1-\eta)^3}\right] + \left(\frac{1}{N_i} + \frac{1}{N_j}\right)\frac{1}{1-\eta} + \sum\frac{\phi_i}{N_i}\frac{\eta}{(1-\eta)^2} \tag{8}$$

and

$$-\beta\epsilon_{ij}^{app}(\eta) = \beta\bar{\epsilon}_{ij} f_p\frac{u(\eta)}{\eta} + \beta\left(\sum_k \eta_k\{\bar{\epsilon}_{ik} + \bar{\epsilon}_{jk}\}\right) f_p\frac{\partial}{\partial\eta}\left(\frac{u(\eta)}{\eta}\right) + \frac{1}{2}\beta\left(\sum_{kl}\eta_k\eta_l\bar{\epsilon}_{kl}\right) f_p\frac{\partial^2}{\partial\eta^2}\left(\frac{u(\eta)}{\eta}\right) \tag{9}$$

In eq 9, $\bar{\epsilon}_{ij}$ denotes the characteristic i,j interaction parameter and $u(\eta) = (\gamma/C)^4\eta^4 - (\gamma/C)^2\eta^2$ with $\gamma = 1/\sqrt{2}$, and $C = \pi/6$ describes the density dependence of attractive nonbonded interactions. The numeric prefactor f_p associated with $u(\eta)$ is simply $f_p = 4$. Finally, the equilibrium bulk density η ($= \sum\eta_i$) is determined at a given set of temperature and pressure from the following CS equation of state: [49,57]

$$\beta P = \frac{f_p}{2}\frac{\beta\sum\phi_i\phi_i\bar{\epsilon}_{ij}}{v^*}\cdot\eta^2\frac{\partial u(\eta)}{\partial\eta} + \frac{1}{v^*}\left[\frac{3}{2}\frac{(\eta^2+\eta^3)}{(1-\eta)^3} + \sum\frac{\phi_i}{N_i}\frac{\eta+\eta^2/2}{(1-\eta)^2}\right] \tag{10}$$

The density η_i of individual components is computed as $\phi_i\eta$.

The evolution of order parameters is given in the spirit of the deterministic time-dependent Ginzburg−Landau equation as

$$\psi_i(\vec{r}, t + {}^1/_2) = \psi_i(\vec{r}, t) - M\frac{\delta\beta F}{\delta\psi_i(\vec{r}, t)} \tag{11}$$

where M is the empirical mobility parameter. The Gaussian random noise can later be taken into consideration for the stochastic approach. After each half time step, a treatment for material balance is undertaken by rescaling local densities ($\eta_i(t+1) = \eta_i(t+{}^1/_2)\cdot[\eta_i\int d\vec{r}/\int d\vec{r}\eta_i(t+{}^1/_2)]$) and then recalculating order parameters ($\psi_i(t+1) = \eta_i(t+1) - \eta_i$). In some simulation runs, a simpler procedure ($\psi_i(t+1) = \psi_i(t+{}^1/_2) - \int d\vec{r}\psi_i(t+{}^1/_2)/\int d\vec{r}$) is employed. This time-splitting scheme of the order parameter evolution works out well in the present dissipative dynamics.

The phase behavior of block copolymer films with finite thickness can also be analyzed with the present simulations. Surface interaction can be treated as the external field term, $-\int d\vec{r}H_j\,\delta(x - L_i)\psi_j$, added into the free energy functional βF, where H_j describes the extremely short-ranged surface−monomer interactions acting at the position $x = L_i$. It should be noted that the order parameters of the films in the film thickness direction are described by cosine series only in order to account for reflecting boundary conditions. In the other directions, both cosine and sine series are required to support periodic boundary conditions. Mathematically stated, the order parameter is transformed into

$$\psi_j(q_x, q_y, q_z) = \int dydz\int_{L_1}^{L_2} dx\psi_j(x, y, z)\, e^{iyq_y}\, e^{izq_z}\cos(xq_x) \tag{12}$$

where $q_x(L_2 - L_1)/2\pi = 0, \pm1, \pm2$, etc. Block copolymer melts are, of course, subject to periodic boundary conditions in all directions.

Simulations for Various Copolymer Systems

The formulated free energy functional is now applied to simulate stable or metastable ordered patterns for various block copolymer systems. Prior to displaying illustrative simulation results, let us first review some important aspects of the analytical Landau approach for compressible diblock copolymers[51,53] in order to help us to understand simulations. It is often useful to operate the second-order vertex function to

$$\bar{\Gamma}_{ij} = S_{kl}^{-1}\, M_{ki}^{-1}\, M_{lj}^{-1} \tag{13}$$

where the matrix M_{ij} is defined as

$$[M_{ij}] = \begin{bmatrix} \frac{1}{2\eta} & -\frac{1}{2\eta} \\ 1 & 1 \end{bmatrix} \tag{14}$$

An effective Flory-type interaction parameter χ_F for compressible block copolymers was defined from the following equation:

$$v^*\cdot\det(\bar{\Gamma}_{ij})/\eta\bar{\Gamma}_{22} = v^*\cdot\sum\eta S_{ij}^0/\det(S_{ij}^0) - 2\chi_F = 2\chi_s - 2\chi_F \tag{15}$$

It was shown that χ_F can be divided into two contributions as $\chi_F = \chi_{app} + \chi_{comp}$. The former χ_{app} is given by $\chi_{app} = \beta\Delta\bar{\epsilon}\cdot f_p/2\cdot|u(\eta)|$, where $\Delta\bar{\epsilon}$ is the exchange energy between $\bar{\epsilon}_{ij}$'s as $\Delta\bar{\epsilon} \equiv \bar{\epsilon}_{AA} + \bar{\epsilon}_{BB} - 2\bar{\epsilon}_{AB}$. The χ_{app} can then be viewed as the exchange energy density. The remaining χ_{comp} is given as $\chi_{comp} = \bar{\Gamma}_{12}^2/2\eta\bar{\Gamma}_{22}$. It was shown in our previous works[51,53−55] that $\bar{\Gamma}_{12}$ ($\propto[\bar{\epsilon}_{AA} - \bar{\epsilon}_{BB}]$ at $\phi_A = 0.5$) and, thus, χ_{comp} represents the compressibility difference between block components in a given system. A composite parameter $N\chi_F$ claims the so-called relevant parameter for the phase behavior of the given compressible copolymer instead of $N\chi$ in the incompressible situation.

In the case that A block is less compressible, an approximate Landau free energy at a dominant wavenumber, $|\vec{Q}| = Q$, can

be written as

$$\beta[F - F_0]/\eta \approx [2\chi_s - 2\chi_F]\cdot\bar{\psi}_n(1)^2 - \left[\frac{a_n}{N} + \frac{\Delta\bar{\Gamma}_{12}}{\eta\bar{\Gamma}_{22}}\right]\bar{\psi}_n(1)^3 + \frac{b_n}{N}\bar{\psi}_n(1)^4 \quad (16)$$

where $\bar{\psi}_n(1)/\sqrt{n}$ describes the amplitude of a coupled order parameter $\bar{\psi}_1(\vec{r})$ ($\equiv (\psi_1 - \psi_2)/2\eta$) for periodically patterned ordered systems characterized by n reciprocal lattice vectors $\vec{Q}$'s. The symbols a_n and b_n are identical with α_n and β_n (eqs V-10, 11, 14, 15, and 26 in ref 9) for a proper microphase morphology, respectively, in the Landau free energy by Leibler for incompressible UODT diblock copolymer melts.[9] It is clear from eq 16 that the mean-field spinodal satisfies $N\chi_F(Q) = N\chi_s(Q)$ and thus takes the universal value of 10.495 for symmetric diblock copolymers regardless of compressibility. Another coupled order parameter $\bar{\psi}_2(\vec{r})$ ($\equiv \psi_1 + \psi_2 = -\langle\delta\eta_f(\vec{r})\rangle$) is necessary to describe the fluctuations in free volume fraction $\eta_f(\vec{r})$. The $\bar{\psi}_2(\vec{r})$ was then intuitively divided into two terms as $\psi_2 = \zeta + \xi$. The former stands for the preference of free volume for a more compressible block if there is a compressibility difference between blocks. The latter accounts for the screening of unfavorable interactions between dissimilar monomers at the A−B interfaces. The ζ thus fluctuates with the wavenumber Q, whereas ξ does with the wavenumber $2Q$. The Δ is given by the coupled third-order vertex functions, which are evaluated in the case that the three wave vectors form an equilateral triangle. The amplitudes $\zeta_n/\sqrt{n}$ and $\xi_n/\sqrt{n}$ associated with ζ and ξ are determined by $\bar{\psi}_1(1)$ as a result of minimization as

$$\zeta_n = -\frac{\bar{\Gamma}_{12}^{(2)}}{\bar{\Gamma}_{12}^{(2)}}\bar{\psi}_n(1) - \frac{\Delta}{2\bar{\Gamma}_{22}^{(2)}}\bar{\psi}_n(1)^2 \quad (17)$$

$$\zeta_n = -\frac{\Pi}{2\bar{\Gamma}_{22}^{(2)}(2Q)}\bar{\psi}_n(1)^2 \quad (18)$$

where Π is given by the coupled third-order vertex functions that involve two $\vec{Q}$'s and one $-2\vec{Q}$. All the numerators, $\bar{\Gamma}_{12}$, Δ, and Π, in eqs 17 and 18, are negative as they should. It is shown that $-\Delta\bar{\Gamma}_{12}/\bar{\Gamma}_{22}$ gives a nonvanishing and negative contribution to the free energy for bcc and hex morphologies, if $\bar{\Gamma}_{12}$ is nonzero. This procedure yields the sequence of transition of disorder → bcc → hex → lam with $N\chi_F$ for the entire range of composition again with nonvanishing $\bar{\Gamma}_{12}$. The mean-field continuous transition exists only if the copolymer is symmetric ($a_n \to 0$ as $\phi_A \to 0.5$) and there is no compressibility difference ($\bar{\Gamma}_{12} \to 0$ as $|\epsilon_{AA} - \epsilon_{BB}| \to 0$).[53−55]

We now present simulations for some selected block copolymer melts and films. For all the simulations, the chain sizes of given copolymer systems are chosen to be large enough to stabilize the liquid state at ambient or higher pressure. Here, two-dimensional simulations for A−B diblock copolymers are only performed. The generalization to multiblock copolymers and three-dimensional simulations is, however, straightforward. A simulation box in the units of the unperturbed gyration radius R_g of the copolymers is discretized into 32 × 32 lattice sites. The box sizes can be varied to reduce the free energy or fixed at any values. All the simulations given here start from a random configuration of order parameters unless mentioned otherwise. The computational time depends on the characteristics of a given system. For a typical example of a compressible diblock copolymer with a chain size N of $O(100)$ in a simulation box of $\sim 3R_g \times 3R_g$, a clearly developed structure, with the box dimensions varied to release the strain energy, requires several hours on a personal computer. As a first case, a symmetric diblock copolymer with no compressibility difference between constituents ($\bar{\Gamma}_{12}, \chi_{comp} \to 0$) is considered. Equation 16 is then formally identical to Leibler's incompressible Landau energy except more complicated χ_F ($= \chi_{app}$), replacing simple Flory's χ. Therefore, eq 16 and Leibler's Landau energy reveal common features such as the existence of a continuous transition. The presence of free volume, however, lends a significant difference to eq 16 so that it yields properties pertinent to compressible systems such as barotropicity. Ordering is induced upon pressurization as the exchange energy density χ_{app} increases with the increased density. The pressure dependence of transition temperatures is typically of 20−30 K/100 MPa.[51−53] The intuitive input of the free volume fluctuations in our analytical theory can be compared with the simulation results. To characterize a given block copolymer system, the compressible RPA by Cho requires various molecular parameters, which include the self-interaction parameter $\bar{\epsilon}_{ii}$, the monomer diameter σ_i, the chain size N_i for pure polymers, and the parameter $\bar{\epsilon}_{ij}$ for cross interaction between different polymers. Those parameters for A block are chosen as follows: $\sigma_1 = 4.04$ Å, $\bar{\epsilon}_{11}/k = 4107.0$ K. As was shown in our previous publications[49−51] for the compressible RPA, this set of parameters represents polystyrene. To ensure that there is no compressibility difference between blocks, the identical set of parameters is assumed to represent B block: $\sigma_2 = \sigma_1$, $\bar{\epsilon}_{22} = \bar{\epsilon}_{11}$. The cross interaction parameter $\bar{\epsilon}_{12}$ of $0.99534(\bar{\epsilon}_{11}\bar{\epsilon}_{22})^{1/2}$ is used here to yield an unfavorable $\Delta\bar{\epsilon}/k = 38.277$. The total chain size is chosen as $N = N_1 + N_2 = 400$. The subdivided order parameter ζ for compressibility difference is then vanishing. Free volume act as a neutral solvent to screen the unfavorable energetics, in particular, at the A−B interfaces.[51,53] Figure 1 shows the simulation results of such a system at 549 K and at 0.1 MPa.

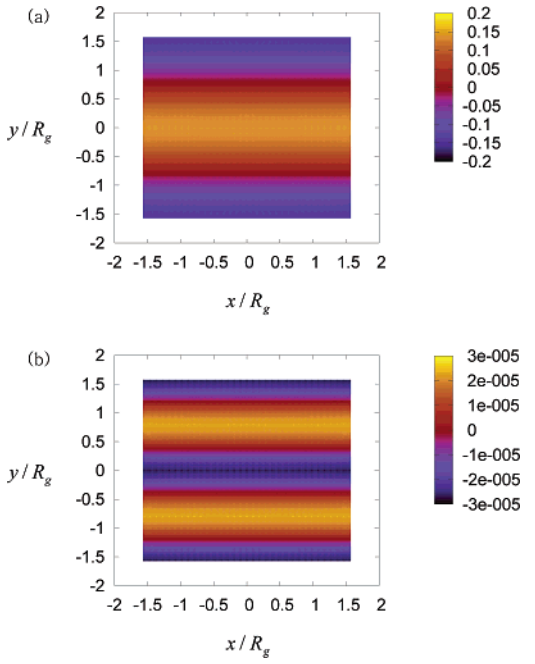

Figure 1. Two-dimensional density plots of $\psi_A(\vec{r})$ for species A (a) and of $\langle\delta\eta_f\rangle = -(\psi_A + \psi_B)$ for free volume fluctuations (b) in the case of a symmetric A-*b*-B copolymer with no compressibility difference. The simulation is performed for the copolymer at 0.1 MPa with $N\chi_F(Q) = 11.2711$. It is shown that excess free volume is located at the interfaces to screen the unfavorable energetics. All of the axes are scaled by the unperturbed gyration radius of the copolymer.

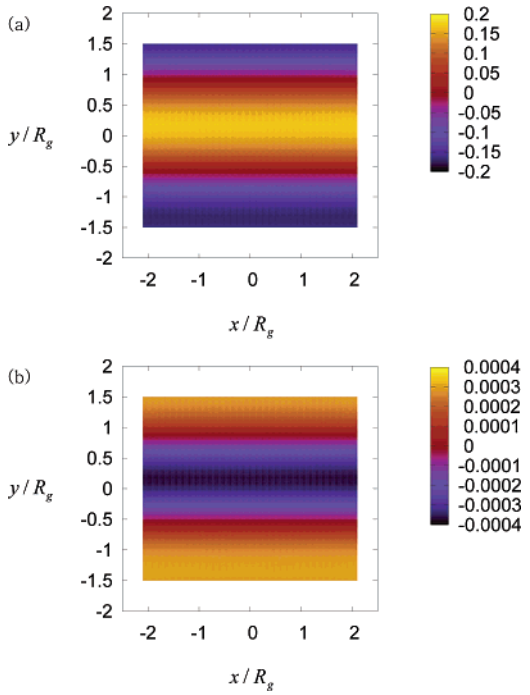

Figure 2. Two-dimensional density plots of $\psi_A(\vec{r})$ for polystyrene (a) and of $\langle \delta\eta_f \rangle = -(\psi_A + \psi_B)$ for free volume fluctuations (b) in the case of a symmetric SBD diblock copolymer. The simulation is performed for the copolymer at 0.1 MPa with $N\chi_F(Q) = 11.7206$. It is seen that free volume fluctuates out of phase with the fluctuations of the less-compressible polystyrene. Free volume fluctuations for screening are hidden.

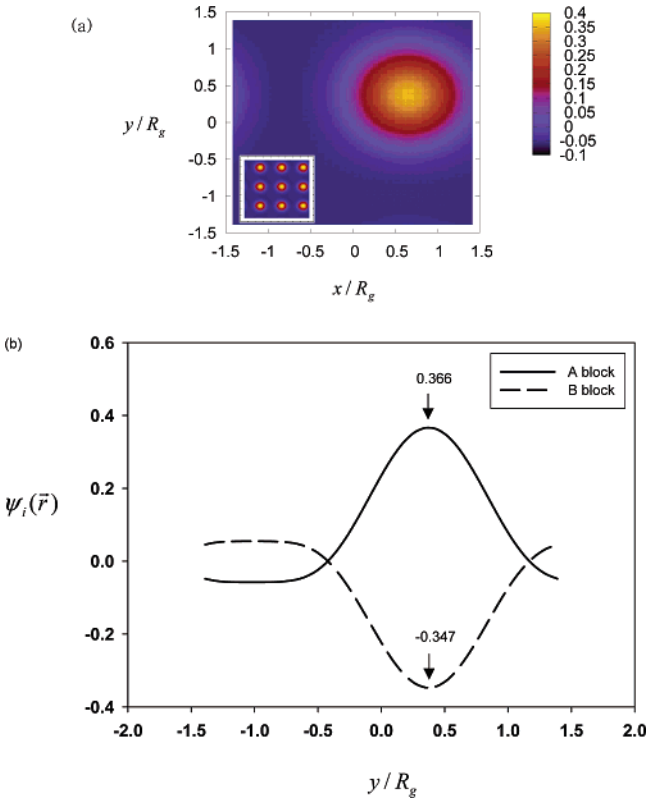

Figure 3. Density plot of the isosurface for a LDOT diblock copolymer with $N = 2000$ and with a highly asymmetric composition ($\phi_A = 0.15$) at 350 K and at 0.1 MPa. The dimensions of the simulation box are allowed to vary in order to release the strain energy. Inside plot (a), the unit cell is extended using the periodic boundary condition to reveal the cubic packing of spheres, which signifies the most favored bcc structure in the given condition of ϕ_A and $N\chi_F$. In plot (b), the order parameters, $\psi_A(\vec{r})$ and $\psi_B(\vec{r})$, at $x/R_g = 0.620$ are drawn.

In this condition, the copolymer experiences the effective Flory interaction $N\chi_F = 11.2711$. It is seen that a lamellar pattern is obtained in plot (a), while excess free volume in plot (b) is located at the interface with half the periodicity of lamellae. The simulation results are, therefore, supportive of our intuitive treatment of free volume fluctuations.

Our second sample materials are real and typical diblock copolymers such as polystyrene-*b*-polybutadiene (SBD) or polystyrene-*b*-poly(methyl methacrylate) (SMMA), with both unfavorable energetics and small compressibility difference. As the small compressibility difference yields nonvanishing $\bar{\Gamma}_{12}$ and Δ, a weak first-order transition prior to $N\chi_F$ at spinodals becomes possible even for symmetric copolymers in the mean-field situation. [53] Both ζ for compressibility difference and ξ for screening are required in this case. As seen in eqs 17 and 18, the differences in the order of $\bar{\psi}_n(1)$, in particular, imply that $\zeta_n \gg \xi_n$. As was employed in our previous publications,[49,51] SBD copolymer is characterized by the above set of parameters for polystyrene and the following one: $\sigma_2 = \sigma_1$, $\bar{\epsilon}_{22}/k = 4065.9$ K. The compressibility difference between constituents is mostly determined by the difference in self-interaction parameters; $|\bar{\epsilon}_{11} - \bar{\epsilon}_{22}|$ per one theoretical monomer ($\sigma = 4.04$ Å) is only ~1% of $\bar{\epsilon}_{11}$. The cross interaction parameter $\bar{\epsilon}_{12}$ is estimated from the corresponding blend phase behavior as $0.995\,65(\bar{\epsilon}_{11}\bar{\epsilon}_{22})^{1/2}$ to yield an unfavorable $\Delta\bar{\epsilon}/k = 35.655$ K.[59] For the symmetric copolymer of $N = 300$, which gives the molecular weight (MW) of ~15 000, the simulation run at 400 K and at 0.1 MPa shows the lamellar morphology, as seen in the plot (a) of Figure 2. The effective Flory interaction in this case reads $N\chi_F(Q) = 11.7206$ with $N\chi_{app} = 11.7068$. The pressure response of the transition temperatures is similar to the previous case because $N\chi_{comp}$ is small. The excess free volume in the plot (b) of this figure is, however, mostly out of phase with the order parameter for the less compressible component (polystyrene), which has the larger $\bar{\epsilon}_{ii}$. The simulation results are harmonious with our analytical theory. As $\zeta_n \gg \xi_n$, the fluctuations associated with the screening are hidden in those associated with the compressibility difference. This inequality explains the simulated free volume fluctuations apparently reveal the characteristic of ζ.

It has been shown that the simulation results support the analytical Landau energy in eq 16. In fact, those two approaches are complementary to each other. While the previous two cases deal with typical UODT character, one can also test a group of materials that reveal ordering reversely upon heating, i.e., LDOT character. This peculiar phase behavior is exhibited by some block copolymers containing polystyrene.[6,39,40] The LDOT behavior is driven entropically either by compressibility difference between constituent blocks[50] or by specific interactions between dissimilar monomers.[55,60] Polystyrene-*b*-poly(vinyl methyl ether) is considered to belong to the former case,[50] while the homologous series of polystyrene-*b*-poly(lower *n*-alkyl methacrylate) with ethyl to *n*-pentyl pendant groups to the latter.[55] As an illustration of the former case, a LDOT symmetric diblock copolymer is to be simulated with the set of parameters for polystyrene and the following one: $\sigma_2 = \sigma_1$, and $\bar{\epsilon}_{22}/k = 3239.6$ K. Relatively large $|\bar{\epsilon}_{11} - \bar{\epsilon}_{22}|$ significantly contributes to χ_{comp}, which provides the source of microphase separation. The cross interaction parameter $\bar{\epsilon}_{12}$ of $1.008\,00(\bar{\epsilon}_{11}\bar{\epsilon}_{22})^{1/2}$ is used in this case to yield a favorable $\Delta\bar{\epsilon}/k = -6.9759$ K. In the plot (a) of Figure 3, the copolymer with a highly asymmetric composition ($\phi_1 = 0.15$) and $N = 2000$ was simulated at 350 K and at 0.1 MPa. The compressibility driven microphase

separation is shown to yield the cubic packing of spheres signifying the most favored bcc morphology at the given composition and the segregation level. This copolymer reveals $N\chi_F(Q) = 42.9575$ at $\phi_1 = 0.15$. The exchange energy density χ_{app} is negative, as $\chi_{app} \propto \Delta\bar{\epsilon}$. This χ_{app} is compensated by larger and positive χ_{comp}, where $N\chi_{comp}$ reads 60.2167 at the given composition. It is seen in plot (b) of this figure that the ratio of amplitudes for the two order parameters, $\psi_n(A)/\psi_n(B)$, vividly deviates from 1; $\psi_n(A)/\psi_n(B) \approx 1.05$. This number corresponds to the ratio of A and B homopolymer densities, as $\eta(\phi_A \rightarrow 1) = 0.4325$ and $\eta(\phi_A \rightarrow 0) = 0.4135$. This phenomenon is indeed observable for all copolymer systems with finite compressibility difference. The latter case of LDOT behavior driven by specific interactions can also be analyzed with the present field-theoretic simulation method by adopting a Sanchez−Balasz-type approach to treating cross-interaction parameters,[55,61] which is not pursued in this work.

One of the merits of the present field-theoretic simulation method is its capability to describe pressure effects on nanostructured materials. Materials in the ordered state show higher elastic resistance to shear than in the disordered state. Baroplastic materials in particular respond to hydrostatic pressure to enhance phase mixing. The changes in the transition temperatures reach up to 100−700 K/100 MPa in an absolute sense. As the normal processing condition always involve the exertion of pressure, this issue is important in designing and controlling self-assembled nanostructures. LDOT systems are usually baroplastic, and as a result, the order−disorder transition under pressure is further increased to a higher temperature region.[41,42] Some UODT systems such as polystyrene-*b*-poly(*n*-hexyl methacrylate),[42] polystyrene-*b*-poly(*n*-butyl acrylate),[46] and polystyrene-*b*-poly(2-ethylhexyl acrylate)[46] can be categorized as having this property. The loop-forming polystyrene-*b*-poly(*n*-pentyl methacrylate) yields the unprecedented pressure coefficient of transition temperatures over 700 K/100 MPa.[48] Consider a diblock copolymer with the parameter set of polystyrene and the following one can be chosen for relevant simulations: $\sigma_2 = \sigma_1$, and $\bar{\epsilon}_{22}/k = 3000$ K. The cross interaction parameter $\bar{\epsilon}_{12}$ of 0.996 $70(\bar{\epsilon}_{11}\bar{\epsilon}_{22})^{1/2}$ that yields an unfavorable $\Delta\bar{\epsilon}/k = 109.910$ K is used here to simulate the UODT character. The total chain size is taken to be somewhat small as $N = N_1 + N_2 = 100$, and the composition is set to $\phi_A = 0.3$. As pressure is increased, the unfavorable contact interactions or χ_{app} increases due to the increased density. However, the given compressibility difference and thus χ_{comp} are greatly suppressed with pressure on the contrary. Such a pressure dependence of $N\chi_{app}$ and $N\chi_{app}$ at $T = 400$ K is depicted in plot (a) of Figure 4. The overall action then enhances the miscibility upon pressurization. The effective Flory interaction $N\chi_F(Q)$ at 400 K changes from 16.0168 at 0.1 MPa to 14.5307 at 100 MPa and then to 14.0549 at 200 MPa. It is obtained that the mean-field spinodal pressure at this temperature is $P_s = 87$ MPa. The plots (b) and (c) of this figure depict the evolved patterns for the copolymer system at 36.73 MPa ($<P_s$) and at 100 MPa ($>P_s$), respectively. In the former case, $N\chi_F(Q)$ reads 15.2260. As can be seen in those plots, the hex pattern is shown in the former case, whereas disordering occurs in the latter.

Surface ordering phenomena in block copolymer films are of practical importance due to the applicability of nanopatterning on a substrate to microelectronics. The current simulations can be performed with a substrate surface exerting an external field. To illustrate this, let us consider two cases of barotropic UODT systems. The first illustration is the symmetric SMMA copolymer system, which reveals the pressure coefficient of ODT of

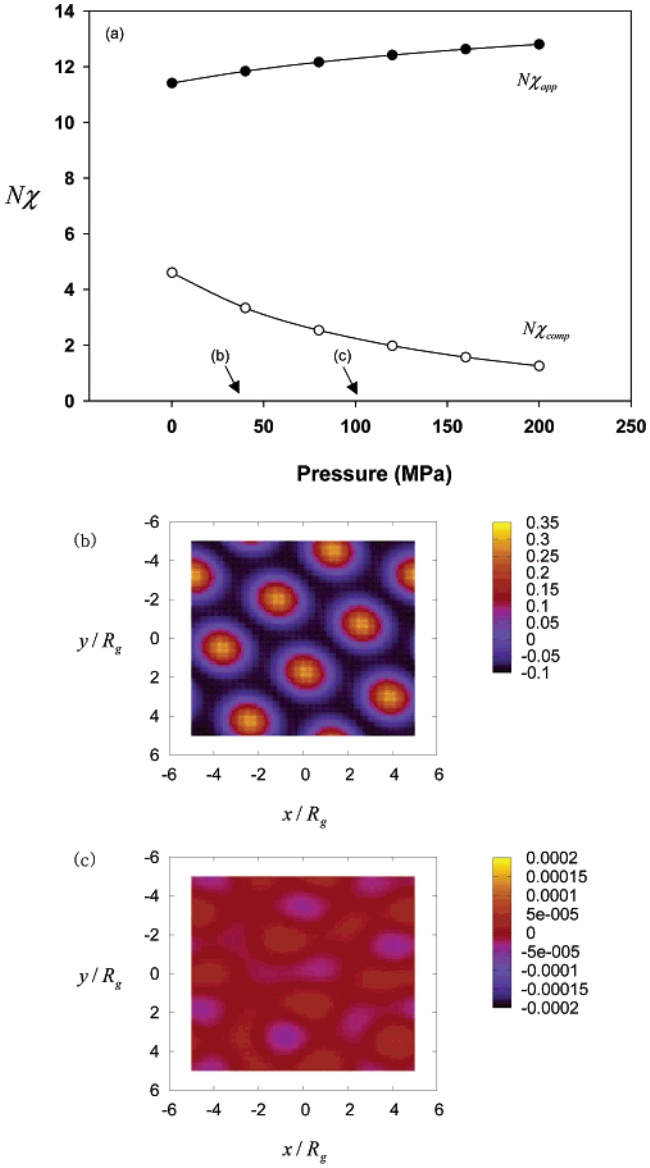

Figure 4. Behavior (a) of $N\chi_{app}$ and $N\chi_{comp}$ plotted against pressure for a baroplastic A-*b*-B copolymer ($\phi_A = 0.3$) at 400 K. The copolymer at 36.73 MPa is shown to be ordered, exhibiting the hex morphology in plot (b). Further pressurization at 100 MPa is found to force the copolymer to be mixed, as seen in plot (c).

∼23 K/100 MPa.[42] SMMA is indeed one of the most frequently used in thin film studies.[62,63] The MMA block is characterized by $\sigma_2 = 3.92$ Å and $\bar{\epsilon}_{22}/k = 4196.8$ K. The cross-interaction parameter $\bar{\epsilon}_{12}$ of 0.997 $52(\bar{\epsilon}_{11}\bar{\epsilon}_{22})^{1/2}$ with the unfavorable $\Delta\bar{\epsilon}/k = 21.0778$ K yields a reasonable estimate for the copolymer phase behavior.[64] The discrepancy in monomer sizes is resolved by employing the average $\sigma = (\sigma_1 + \sigma_2)/2$. The total chain size is chosen as $N = 458.25$, which corresponds to the copolymer with MW of 23 000. The copolymer film is confined between two identical substrates with the thickness of 9.83 in the units of the unperturbed gyration radius R_g. The surface interactions are characterized by $H_1/k = -0.5$ and $H_2/k = 0.2$ K, which favors the MMA block. In this case, the simulation run starts from a sinusoidal profile possessing the amplitude of ∼0.005, with the styrene block contacting both surfaces. Figure 5 depicts the annealed film at 415 K (a) and 380 K (b). Pressure is fixed at 0.1 MPa. The effective Flory interaction $N\chi_F(Q)$ in each case reads 10.2482 and 11.3734, respectively. With the chosen set of molecular parameters, the bulk copolymer melts exhibit the

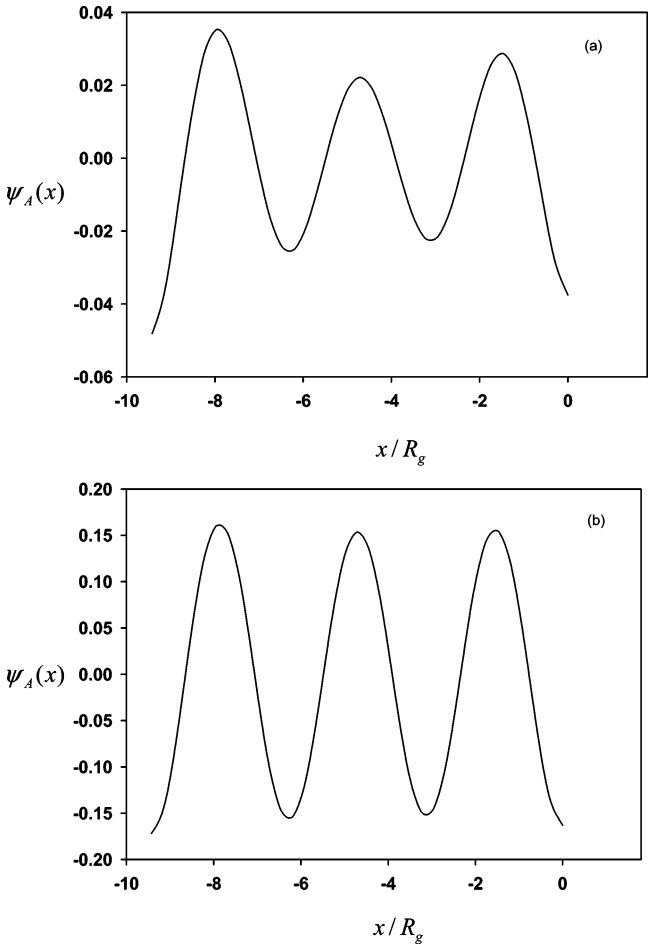

Figure 5. One-dimensional order parameter $\psi_A(x)$ of a symmetric SMMA copolymer film of MW = ~23 000 with 9.83 R_g thick in the presence of surface interactions, which are set to $H_1/k = -0.5$ and $H_2/k = 0.2$ K at both sides. It is seen that MMA block is in contact with the substrates due to the selected surface interactions. Simulations for the two plots (a) and (b) are performed above and below the mean-field order−disorder transition, respectively. Pressure is set to 0.1 MPa.

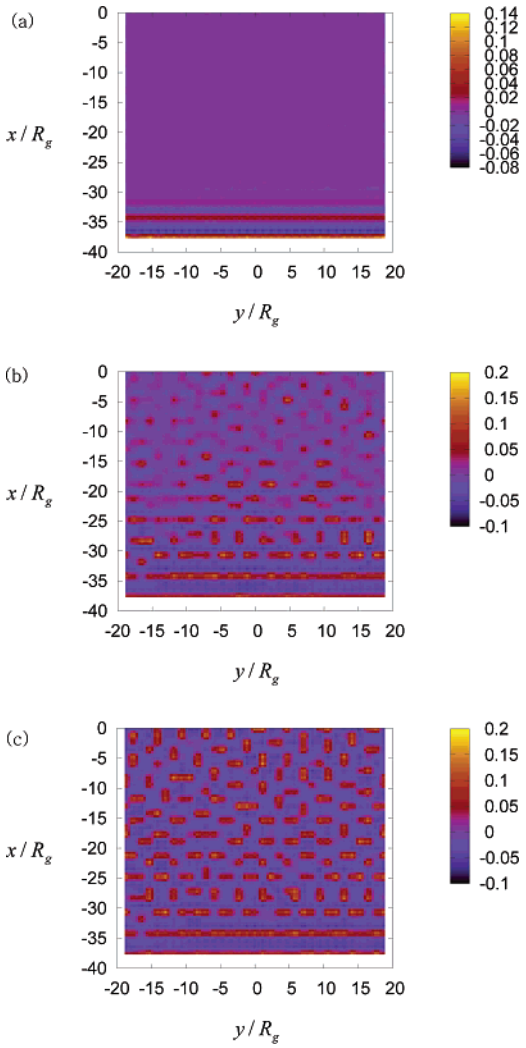

Figure 6. Time evolution of the pattern formation for an ordered asymmetric A-*b*-B copolymer film ($\phi_A = 0.3$) of $N = 100$ with no compressibility difference at 400 K. Pressure is fixed to 0.1 MPa. The film thickness is chosen as 37.70 R_g. The surface interaction strength is set to $H_1/k = 2$ and $H_2/k = -5$ K at $x/R_g = -37.70$ and $H_1/k = H_2/k = 0$ K at $x/R_g = 0$. The simulation times for plots (a−c) are as follows: (a) 168, (b) 690, and (c) 2200 (in arbitrary units).

mean-field order−disorder transition temperature of 406 K at ambient pressure. As seen in the plot (a) of this figure, the substrate induces surface ordering, which eventually leads to phase coherence as the segregation propagates through the film thickness direction. It is shown in this plot that the preferred MMA block is now wetting the substrate due to the chosen surface field values. The phase coherent profiles in plot (a) reveal the decaying amplitudes with a temperature-dependent decay length, which is definitely different from those of the copolymer film in the ordered state in plot (b). These simulation results are in accordance with the experiments on the UODT-type SMMA[62,63] and the LDOT-type polystyrene-*b*-poly(*n*-butyl methacrylate)[40] by Russell and co-workers or the neutron reflectivity measurements and an analytical theoretical interpretation on other styrenic LDOT copolymers.[65]

As the second illustration of the phase behavior in block copolymer thin films, let us consider the asymmetric A-*b*-B copolymer at $\phi_A = 0.3$ with no compressibility difference, which is the simplest barotropic system. The chain length is taken to be rather small as $N = 100$. The molecular parameters characterizing the two block components are assumed to be the same as those for the copolymer used in Figure 1. The cross interaction parameter $\bar{\epsilon}_{12}$ is, however, set to a stronger value of $0.980(\bar{\epsilon}_{11}\bar{\epsilon}_{22})^{1/2}$ ($\Delta\bar{\epsilon}/k = 164.28$ K), which yields $N\chi_F = 15.2260$ at a chosen simulation temperatures of 400 K. The copolymer film is confined between two asymmetric substrates with the thickness of 37.70 R_g. The surface field acting at $x/R_g = -37.70$ is characterized by $H_1/k = 2$ and $H_2/k = -5$ K in favor of dispersed A block, and that at $x/R_g = 0$ is assumed to have $H_1/k = H_2/k = 0$ K. The simulation is performed at ambient pressure for this copolymer film having a random configuration in its initial stage. In this condition, the bulk copolymer melt is ordered with the hexagonal pattern. The preferential affinity of the substrate, however, induces a lamellar wetting layer of A block and the subsequent alternating layers, as seen in the plot (a) of Figure 6. As time evolution is progressed, these surface-induced lamellar layers distant from the interacting surface show the hexagonal undulation to form the dispersed phases. In the remaining part of the simulation box, the randomly developed dispersed phases evolve to the random hex pattern. Such simulation results are shown in plots (b) and (c), although the resolution of this figure is rather low. When the surface fields at $x/R_g = -37.70$ are decreased to $H_1/k = 0.2$ and $H_2/k = -0.5$ K, the surface interactions become weaker, so the surface wetting layer and the subsequent lamellae suffer the hexagonal undulation to be dispersed after annealing. These simulation results are compatible with the experimental study by Kramer

and co-workers on the polystyrene-*b*-poly(vinyl pyridine) or its ABA type triblock copolymers.[66] We expect that a three-dimensional extension of this particular simulation with various choices of surface interaction fields results in a richer morphological variety of cylinder-forming block copolymers as in the series of works using DDFT by Sevink and Magerle.[31,32]

The phase behavior of the block copolymer films addresses many interesting scientific issues such as the commensurability of lamellae layering, frustration induced by curved surfaces, and free surface phenomena. In particular, the free surface problem may well be interpreted by the extension of the present tool or an analytical approach based on the compressible RPA because of the proven accuracy of the CS equation-of-state model[49,57] employed here. Baroplasticity in block copolymer films can also be an addition to the issues just mentioned. The reduced apparent Flory χ_F in such films under an applied pressure is expected to yield the tendency of phase coherence reverse to that of ordinary UODT diblock copolymer films. The simulation results in Figures 5−6 for block copolymer films are primitive but still suggestive of the capability of the present method in relevant studies. More elaborate analyses on the baroplasticity and other issues mentioned above for block copolymers in a confined geometry will be given in our future works.

We have shown the field-theoretic simulations based on the compressible RPA, which suits simulation studies of compressible block copolymer systems. The current simulation method has the definite advantage over our previous analytical theory to study self-assembly behavior and its pressure responses for copolymers in a solvent, either monomeric or polymeric, where a priori guesses of morphologies are unavailable. The structure factors in eq 5 need to be changed to describe such systems. The effects of pressure on micellar formation and dissolution can in particular be investigated with this simulation tool in a visual way. There could be a number of improvements on the present simulation method. For the diblock case, the free energy functional in eq 2 can adopt a Ohta−Kawasaki type analysis[67] for higher-order vertex terms. Their formulation should, of course, be generalized to accommodate multiple order parameters. This procedure would yield a more precise description of the phase behavior in the vicinity of the mean-field spinodals than the present approach with eq 5. As RPA-based free energy functionals yield the square-gradient coefficients with global densities, a way to incorporate locality in those coefficients such as Doi et al.'s recent treatment[37] may need to be devised for us to provide a better description of the copolymer phase and interfacial behavior in the strong segregation regime. The convection term can be added to the dissipative dynamics equations to study the phase behavior of copolymers under flow.[21] For baroplastic materials, this improvement is important in simulating flow problems in order to design an efficient manufacturing process.

Concluding Remarks

A simple field-theoretic simulation method combined with the recently introduced compressible RPA theory has been developed here to understand the variety of nanoscale self-assembly behaviors and their pressure responses for compressible block copolymer systems. Finite compressibility is described by the effective RPA interactions that are included in the free energy functional for the dissipative dynamics to account for the excluded volume and the attractive nonbonded interactions. Input molecular information characterizing a given copolymer is typical of equation-of-state parameters such as self-and cross-interaction parameters, monomer sizes, and chain sizes. Stable or metastable morphologies for given copolymer systems were shown to be yielded without any presumed symmetry over a wide range of temperature−pressure−composition space. Copolymer systems with the LDOT character as well as the conventional UODT character were all simulated by using the present tool. It was shown that barotropicity and baroplasticity in many copolymer systems can also be studied with this new method that accommodates finite compressibility. It was also demonstrated that, not only bulk copolymer melts, but also copolymers in confined geometry, can be simulated to understand the experimentally observed pattern formation. The current theory may be extended to simulate the self-assembly behavior of multiblock copolymers with diverse molecular architectures and also of block copolymers in a solvent covering from complex patterns to micellar structures.

Finally, it needs to be re-emphasized that the present field-theoretic simulation method enables us to study various nanoscale morphologies and phase separation kinetics for copolymer systems in a vast processing window. The capability to treat the effects of pressure on the copolymer phase behavior in particular will prove useful in designing and manufacturing nanostructured materials aimed at desired applications.

Acknowledgment. This work was supported by the Korea Research Foundation Grant (KRF-2005-013-D00020). J.C. acknowledges Dr. Y. Bohbot-Raviv for sharing the code for incompressible block copolymer systems.

References and Notes

(1) Aggarwal, S. L. *Block Copolymers*; Plenum Press: New York, 1970.
(2) Goodman, I., Ed. *Developments in Block Copolymers-I*; Applied Science Publishers: New York, 1982.
(3) Holden, G.; Legge, N. R.; Quirk, R. P.; Schroeder, H. E., Eds. *Thermoplastic Elastomers*; Hanser: New York, 1996.
(4) Hamley, I. W. *The Physics of Block Copolymers*; Oxford University Press: New York, 1998.
(5) Bailey, T. S.; Hardy, C. M.; Epps, T. H.; Bates, F. S. *Macromolecules* **2002**, *35*, 7007.
(6) Russell, T. P.; Karis, T. E.; Gallot, Y.; Mayes, A. M. *Nature* **1994**, *386*, 729.
(7) Ruzette, A.-V. *Nature Mater.* **2002**, *1*, 85.
(8) Lodge, T. P. *Macromol. Chem. Phys.* **2003**, *204*, 265.
(9) Leibler, L. *Macromolecules* **1980**, *13*, 1602.
(10) Fredrickson, G. H.; Helfand, E. *J. Chem. Phys.* **1987**, *87*, 697.
(11) Mayes, A. M.; Olvera de la Cruz, M. *J. Chem. Phys.* **1991**, *95*, 4670.
(12) Barrat, J.-L.; Fredrickson, G. H. *J. Chem. Phys.* **1991**, *95*, 1281.
(13) Helfand, E. *J. Chem. Phys.* **1975**, *62*, 999.
(14) Hong, K. M.; Noolandi, J. *Macromolecules* **1981**, *14*, 727.
(15) Vavasour, J. D.; Whitmore, M. D. *Macromolecules* **1992**, *25*, 5477.
(16) Matsen, M. W.; Schick, M. *Phys. Rev. Lett.* **1994**, *72*, 2660.
(17) Fredrickson, G. H.; Ganesan, V.; Drolet, F. *Macromolecules* **2002**, *35*, 16.
(18) Oono, Y.; Puri, S. *Phys. Rev. Lett.* **1987**, *58*, 836.
(19) Oono, Y.; Bahiana, M. *Phys. Rev. Lett.* **1988**, *61*, 1109.
(20) Oono, Y.; Shiwa, Y. *Mod. Phys. Lett. B* **1987**, *1*, 49.
(21) Hamley, I. W. *Macromol. Theory Simul.* **2000**, *9*, 363.
(22) Ren, S. R.; Hamley, I. W. *Macromolecules* **2001**, *34*, 116.
(23) Fraaije, J. G. E. M. *J. Chem. Phys.* **1993**, *99*, 9202.
(24) Maurits, N. M.; van Vlimmeren, B. A. C.; Fraaije, J. G. E. M. *Phys. Rev. E* **1997**, *56*, 816.
(25) Fraaije, J. G. E. M.; van Vlimmeren, B. A. C.; Maurits, N. M.; Postma, M.; Evers, O. A.; Hoffman, C.; Altevogt, P.; Goldbeck-Wood, G. *J. Chem. Phys.* **1997**, *106*, 4260.
(26) Maurits, N. M.; Zvelindovsky, A. V.; Fraaije, J. G. E. M. *J. Chem. Phys.* **1998**, *108*, 2638.
(27) Drolet, F.; Fredrickson, G. H. *Phys. Rev. Lett.* **1999**, *83*, 4317.
(28) It was shown by Fredrickson et al. that MF can be overcome via a sampling method.[17]
(29) Bohbot-Raviv, Y.; Wang, Z.-G. *Phys. Rev. Lett.* **2000**, *85*, 3428.
(30) Wu, Y.; Cheng, G.; Katsov, K.; Sides, S.; Wang, J.; Tang, J.; Fredrickson, G. H.; Moskovits, M.; Stucky, G. D. *Nature Mater.* **2004**, *3*, 816.

(31) Knoll, A.; Horvat, A.; Lyakhova, K. S.; Krausch, G.; Sevink, G. J. A.; Zvelindovsky, A. V.; Magerle, R. *Phys. Rev. Lett.* **2002**, *89*, 035501.
(32) Horvat, A.; Lyakhova, K. S.; Sevink, G. J. A.; Zvelindovsky, A. V.; Magerle, R. *J. Chem. Phys.* **2004**, *120*, 1117.
(33) van Vlimmeren, B. A. C.; Maurits, N. M.; Zvelindovsky, A. V.; Sevink, G. J. A.; Fraaije, J. G. E. M. *Macromolecules* **1999**, *32*, 646.
(34) Sevink, G. J. A.; Zvelindovsky, A. V.; Fraaije, J. G. E. M. *J. Chem. Phys.* **2001**, *115*, 8226.
(35) Sevink, G. J. A.; Fraaije, J. G. E. M.; Huinink, H. P. *Macromolecules* **2002**, *35*, 1848.
(36) Fraaije, J. G. E. M.; Sevink, G. J. A. *Macromolecules* **2003**, *36*, 7891.
(37) Uneyama, T.; Doi, M. *Macromolecules* **2005**, *38*, 196.
(38) Uneyama, T.; Doi, M. *Macromolecules* **2005**, *38*, 5817.
(39) Ruzette, A.-V. G.; Banerjee, P.; Mayes, A. M.; Pollard, M.; Russell, T. P.; Jerome, R.; Slawecki, T.; Hjelm, R.; Thiyagarajan, P. *Macromolecules* **1998**, *31*, 8509.
(40) Mansky, P.; Tsui, O. K. C.; Russell, T. P.; Gallot, Y. *Macromolecules* **1999**, *32*, 4832.
(41) Pollard, M.; Russell, T. P.; Ruzette, A.-V.; Mayes, A. M.; Gallot, Y. *Macromolecules* **1998**, *31*, 6493.
(42) Ruzette, A.-V.; Mayes, A. M.; Pollard, M.; Russell, T. P.; Hammouda, B. *Macromolecules* **2003**, *36*, 3351.
(43) Schwahn, D.; Frielinghaus, H.; Mortensen, K.; Almdal, K. *Phys. Rev. Lett.* **1996**, *77*, 3153.
(44) Frielinghaus, H.; Schwahn, D.; Mortensen, K.; Almdal, K.; Springer, T. *Macromolecules* **1996**, *29*, 3263.
(45) Schwahn, D.; Frielinghaus, H.; Mortensen, K.; Almdal, K. *Macromolecules* **2001**, *34*, 1694.
(46) Gonzalez-Leon, J. A.; Acar, M. H.; Ryu, S. W.; Ruzette, A.-V.; Mayes, A. M. *Nature* **2003**, *426*, 424.
(47) Ryu, D. Y.; Jeong, U.; Kim, J. K.; Russell, T. P. *Nature Mater.* **2002**, *1*, 114.
(48) Ryu, D. Y.; Lee, D. H.; Kim, J. K.; Lavery, K. A.; Russell, T. P.; Han, Y. S.; Seong, B. S.; Lee, C. H.; Thiyagarajan, P. *Phys. Rev. Lett.* **2003**, *90*, 235501.
(49) Cho, J. *Macromolecules* **2000**, *33*, 2228.
(50) Cho, J. *Macromolecules* **2001**, *34*, 1001.
(51) Cho, J. *Macromolecules* **2001**, *34*, 6097.
(52) Cho, J. *Macromolecules* **2002**, *35*, 5697.
(53) Cho, J. *J. Chem. Phys.* **2003**, *119*, 5711.
(54) Cho, J. *J. Chem. Phys.* **2004**, *120*, 9831.
(55) Cho, J. *Macromolecules* **2004**, *37*, 10101.
(56) Freed and co-workers were the first to incorporate finite compressibility into the incompressible RPA by allowing for vacancy. See: (a) McMullen, W. E.; Freed, K. F. *Macromolecules* **1990**, *23*, 255. (b) Tang, H.; Freed, K. F. *J. Chem. Phys.* **1991**, *94*, 1572. (c) Dudowicz, J.; Freed, K. F. *Macromolecules* **1993**, *26*, 213. (d) Freed, K. F.; Dudowicz, J. *J. Chem. Phys.* **1992**, *97*, 2105. (e) Dudowicz, J.; Freed, K. F. *Macromolecules* **1995**, *28*, 6625. Other theories have also been formulated using vacancies as a pseudosolvent in the incompressible treatment. See: (f) Yeung, C.; Desai, R. C.; Shi, A. C.; Noolandi, J. *Phys. Rev. Lett.* **1994**, *72*, 1834. (g) Bidkar, U. R.; Sanchez, I. C. *Macromolecules* **1995**, *28*, 3963. (h) Hino, T.; Prausnitz, J. M. *Macromolecules* **1998**, *31*, 2636. Pair correlation functions and spinodals from the compressible RPA theories were used to explain LDOT behavior driven by the compressibility difference. Our compressible RPA theory is, however, unique in the sense that it does not depend on the widely used pseudosolvent technique.[49−55]
(57) Cho, J.; Sanchez, I. C. *Macromolecules* **1998**, *31*, 6650.
(58) A more thorough way to incorporate compressibility is to start with the effective Edward Hamiltonian with the formulated RPA interaction fields in eq 7 and to build up a field-theoretic simulation method based on SCFT formalism. In an alternative way, the present C−S equation of state model can be combined with the SCFT through the density functional representing density fluctuations as a part of monomer−monomer interaction potential. See: (a) Schmid, F. *J. Phys.: Condens. Matter* **1998**, *10*, 8105. (b) Muller, M.; MacDowell, L. G. *J. Phys.: Condens. Matter* **2003**, *15*, R609.
(59) The estimation of $\bar{\epsilon}_{12}$ is made to fit the cloud points data of PS/PBD blends with molecular weights of 3500 and 2660, respectively. The chosen set of molecular parameters yields the pressure coefficient of the mean-field ODT of 25 K/100 MPa for the asymmetric SBD at $\phi_{PS} = 0.301$ with MW of 20 000,[51] which is harmonious with the experimental results by Stamm and co-workers. See: Ladynski, H.; Odorico, D.; Stamm, M. *J. Non-Cryst. Solids* **1998**, *235*, 491.
(60) Cho, J.; Kwon, Y. K. *J. Polym. Sci., Part B.: Polym. Phys.* **2003**, *41*, 1889.
(61) Sanchez, I. C.; Balazs, A. C. *Macromolecules* **1989**, *22*, 2325.
(62) Anastasiadis, S. H.; Russell, T. P.; Satija, S. K.; Majkrzak, C. F. *Phys. Rev. Lett.* **1989**, *62*, 1852.
(63) Menelle, A.; Russell, T. P.; Anastasiadis, S. H.; Satija, S. K.; Majkrzak, C. F. *Phys. Rev. Lett.* **1992**, *68*, 67.
(64) Leibler's χ is obtained from the recent neutron scattering data of disordered symmetric SMMA (MW of 19 800) with fully deuterated styrene by Ryu, Kim, Cho, and Russell. From such χ, the symmetric SMMA with MW of 22 160 is projected to have the ODT of 393 K at ambient pressure. The chosen $\bar{\epsilon}_{12}$ yields the ODT of 394 and 406 K for the symmetric copolymer with MW's of 22 160 and 2 3000, respectively, in the mean-field analysis. The chosen set of molecular parameters yields the pressure coefficient of the mean-field ODT of ~15 K/100 MPa for SMMA, which is slightly lower than the experimental value. If fluctuation effects are considered, $\bar{\epsilon}_{12}$ needs to be changed to assign the same ODT. The reports on the compressible RPA analyses of these data are in preparation.
(65) Cho, J.; Shin, K. W.; Cho, K. S.; Ryu, D. Y.; Kim, J. K. Manuscript in preparation.
(66) Liu, Y.; Zhao, W.; Zheng, X.; King, A.; Singh, A.; Rafailovich, M. H.; Sokolov, J.; Dai, K. H.; Kramer, E. J.; Schwarz, S. A.; Gebizlioglu; Sinha, S. K. *Macromolecules* **1994**, *27*, 4000.
(67) Ohta, T.; Kawasaki, K. *Macromolecules* **1986**, *19*, 2621.

MA052565R